

Computational modelling for performance improvement of polymer nanocomposites

Łukasz Figiel

**International Institute for Nanocomposites
Manufacturing (IINM), WMG, University of Warwick**

http://www2.warwick.ac.uk/fac/sci/wmg/research/multifunctional_systems/lfigiel

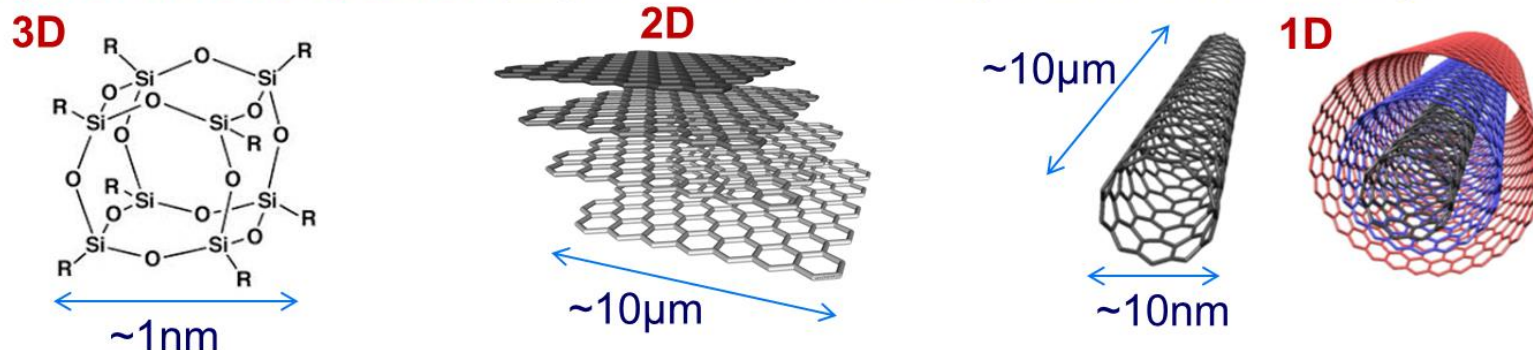


Warwick Centre for Predictive Modelling Seminar

28 May 2015

THE UNIVERSITY OF
WARWICK

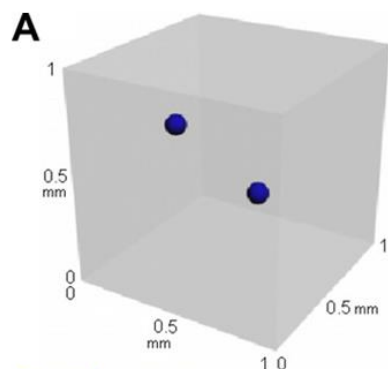
Polymer nanocomposites: polymers filled with nanoparticles at low loadings



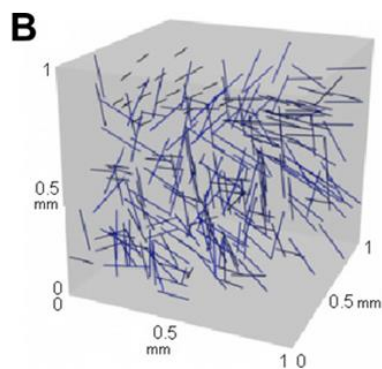
Nanoparticle properties: high stiffness; high conductivities, high surface-to-volume ratio

Challenges: dispersion/distribution and interfacial behaviour

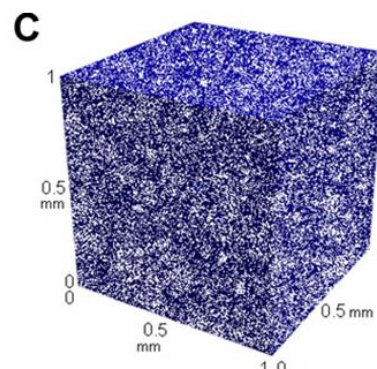
1mm^3 with 0.1% volume fraction



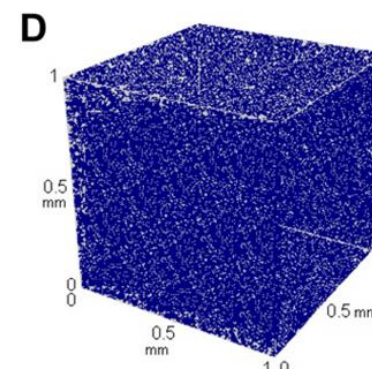
2 spheres
 $100\mu\text{m}$



255 fibres
 $5 \times 200\mu\text{m}$



$\sim 65\text{K}$ platelets
 $7.5\text{nm} \times 45\mu\text{m}$

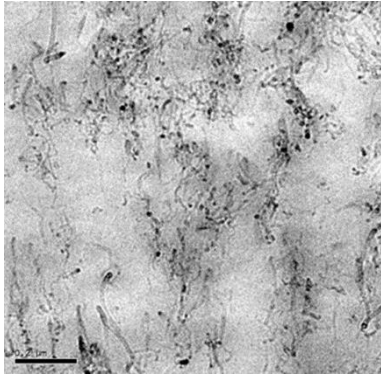


$\sim 442\text{M}$ CNTs
 $12\text{nm} \times 20\mu\text{m}$

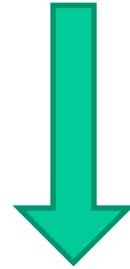
Ma et al. (2010), 41: 1345, Comp. Part A.

IINM Research

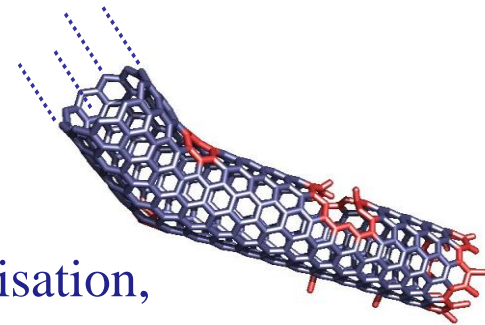
Understanding Materials at the Nanoscale & Linking with Macroscale



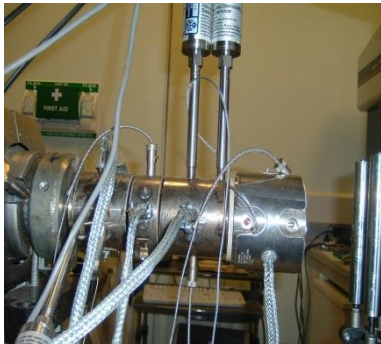
Dispersion & distribution;
Polymer-nanoparticle interactions



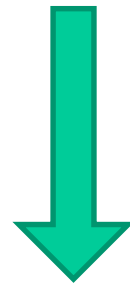
Synthesis, functionalisation, defects



Controlled manufacturability at Scale

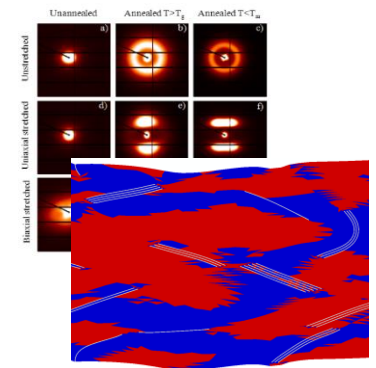


Tracking morphology in primary & secondary processing



In-situ characterisation & modelling

Figure 13



Delivering Material to the End User

IINM Team



Prof Tony McNally
Director
Polymer Science,
Processing,
Functional Materials



Dr Chaoying Wan
Polymer
Chemistry,
Graphene,
Biomimetics



Dr Claire Dancer
Electromagnetic Materials,
Ceramics



Dr Lukasz Figiel
Materials
Modelling,
Mechanics



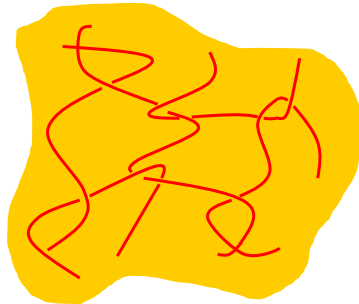
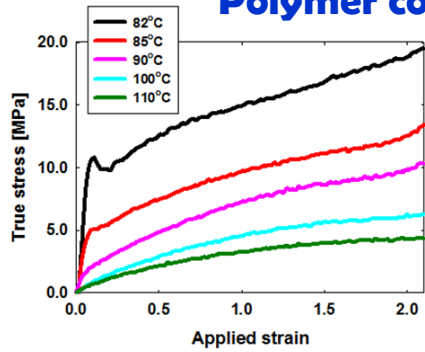
Dr Vannessa Goodship
Polymer Processing



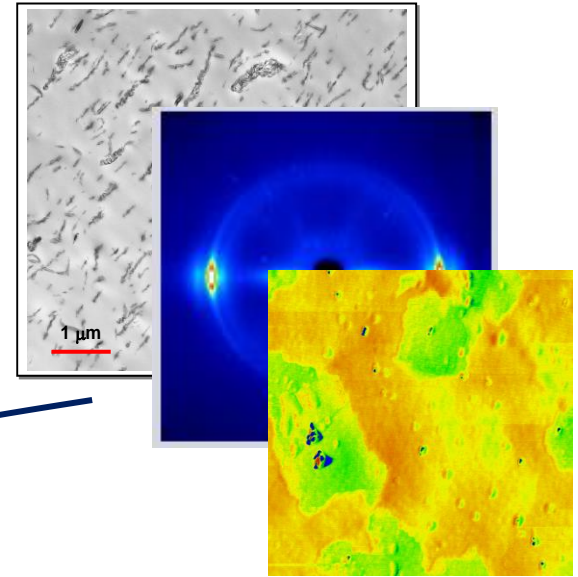
Dr Tara Schiller
Polymer
Characterisation,
Biomaterials

Modelling Methodology: overview

Polymer constitutive law

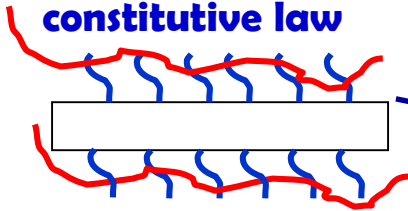


TEM, XRD, AFM

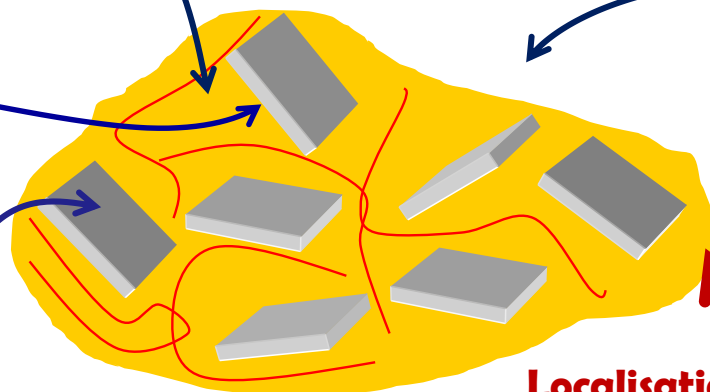


Morphology reconstruction:

Interface/interphase constitutive law



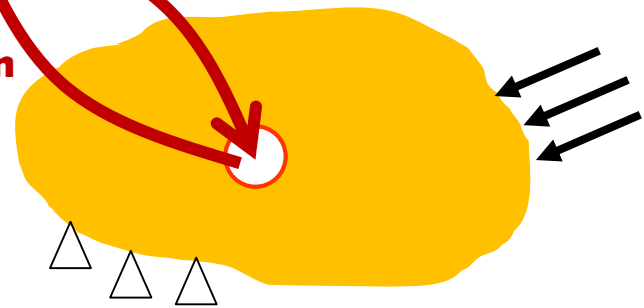
RVE



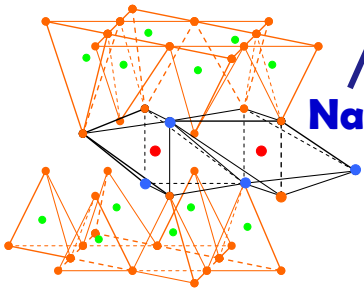
Homogenisation

MACRO

Localisation

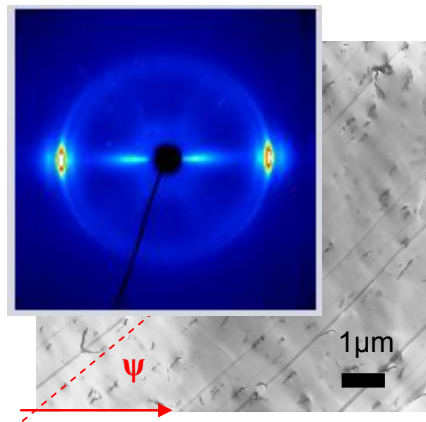


Nanofiller properties

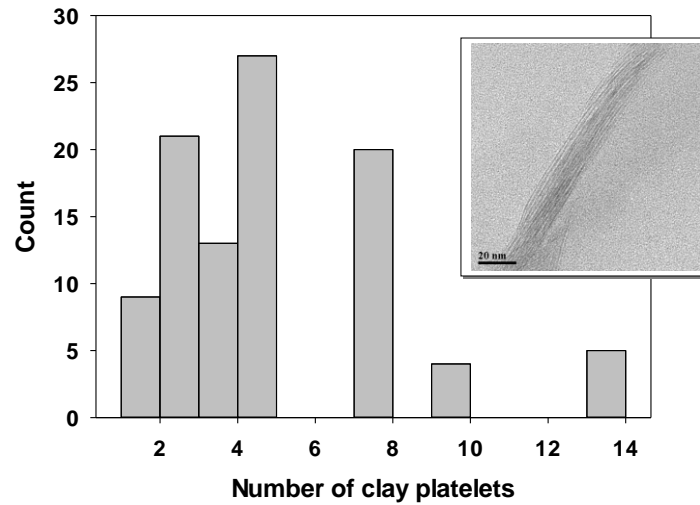


Reconstruction of initial morphology

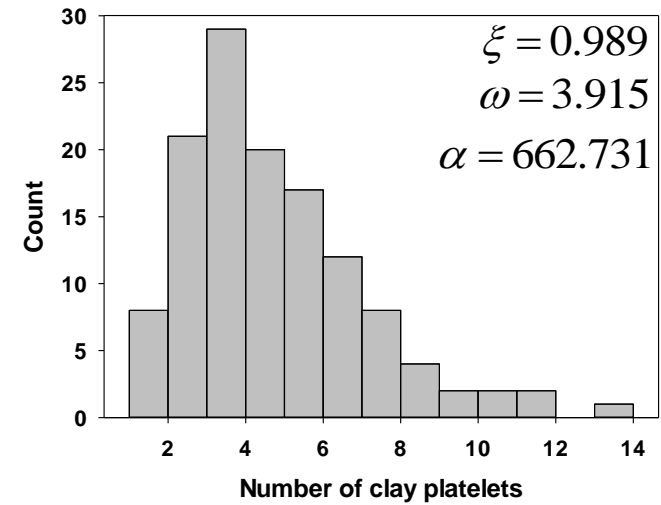
TEM/XRD



Experiment



Digital reconstruction

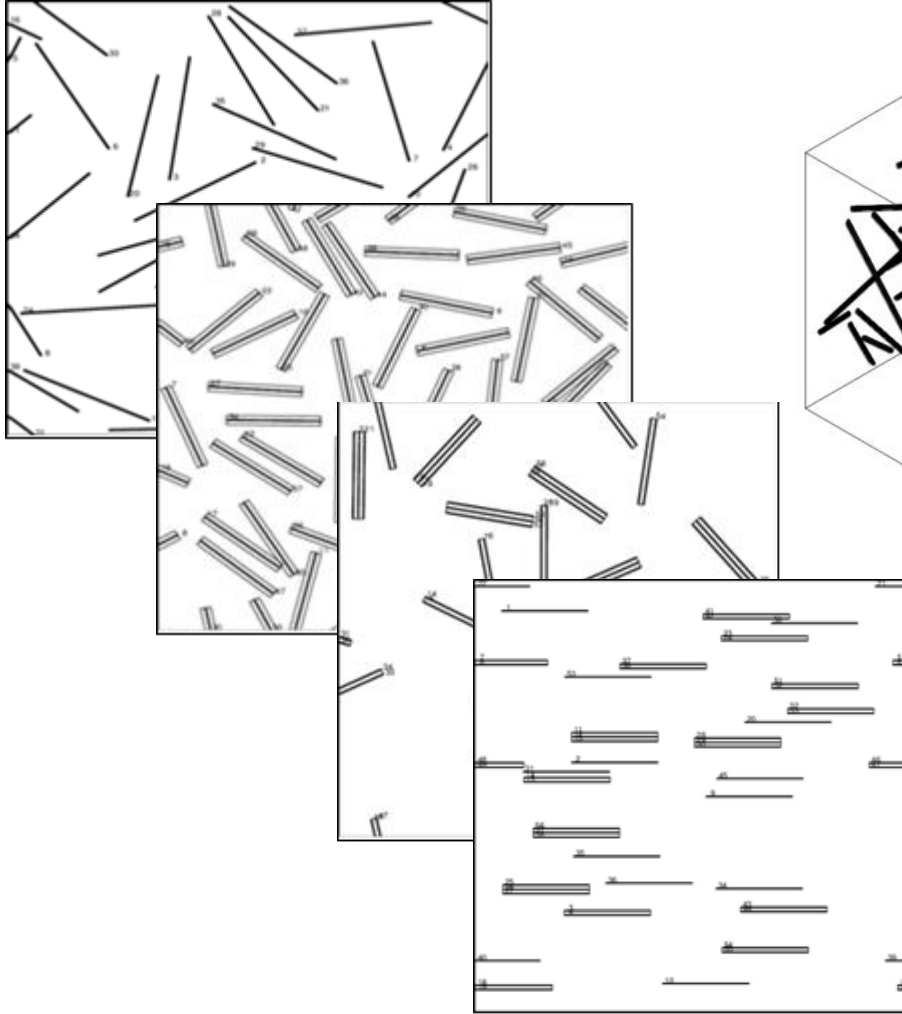


Acceptance-rejection algorithm

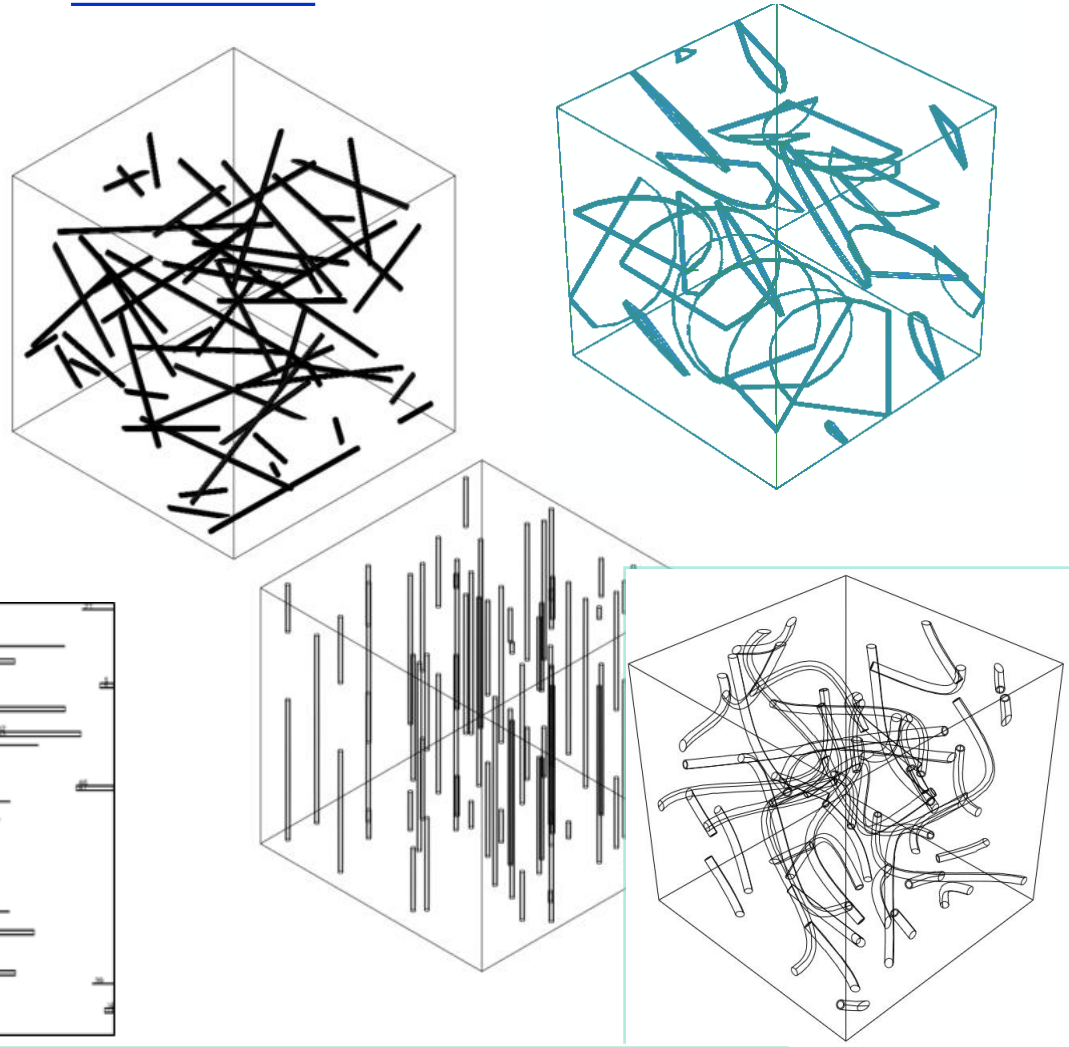
- Draw samples (e.g. orientation) from a given distribution (e.g. skew-Gaussian)
- Intersection/overlap checks
- Ensures global/local periodicity
- Implementation: Fortran (2D) and Python (3D)

Examples of 2D and 3D models

2D models



3D models



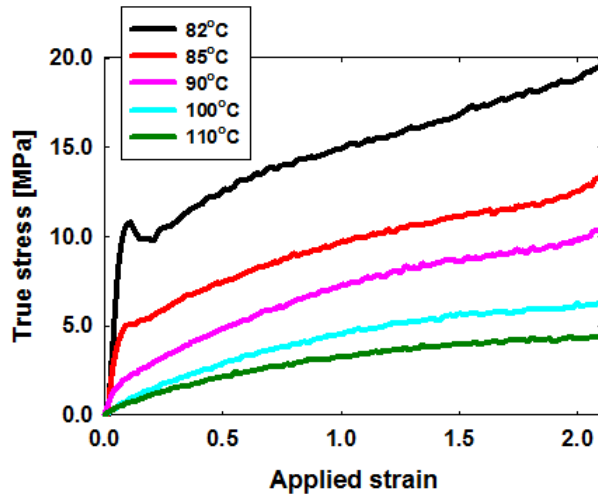
Ł. Figiel/Computational Materials Science 84 (2014) 244–254

D. Weidt, Ł. Figiel/Computational Materials Science 82 (2014) 298–309

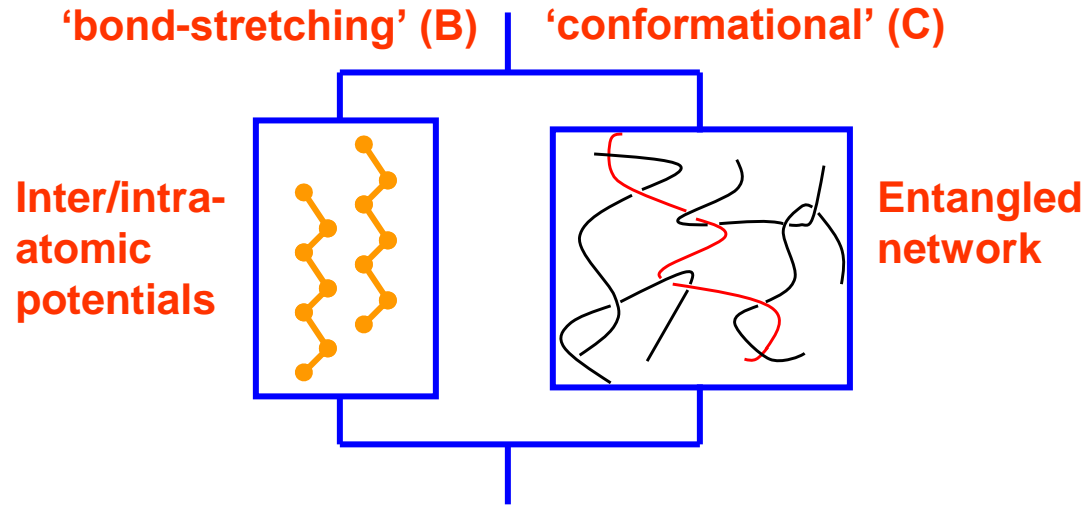
D. Weidt, Ł. Figiel/Composites Science and Technology 115 (2015) 52–59

Constitutive model: polymer matrix

Stress-strain behaviour around Tg - entangled polymer



Glass-rubber model



Total Cauchy stress tensor:

$$\boldsymbol{\sigma} = \hat{\boldsymbol{\sigma}}_B + \hat{\boldsymbol{\sigma}}_C + \sigma_m \mathbf{I} \quad \text{where} \quad \sigma_m = K_B \ln J$$

Bond-stretching (B) stress tensor:

$$\dot{\hat{\boldsymbol{\sigma}}}_B + \frac{\hat{\boldsymbol{\sigma}}_B}{\tau_B} = 2G_B \hat{\mathbf{D}} \quad \text{where} \quad \tau_B = \tau_B(a_T, a_S, a_\sigma)$$

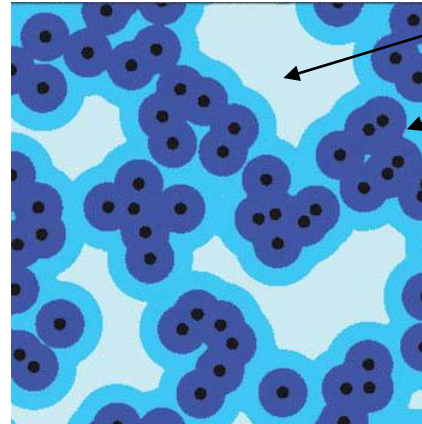
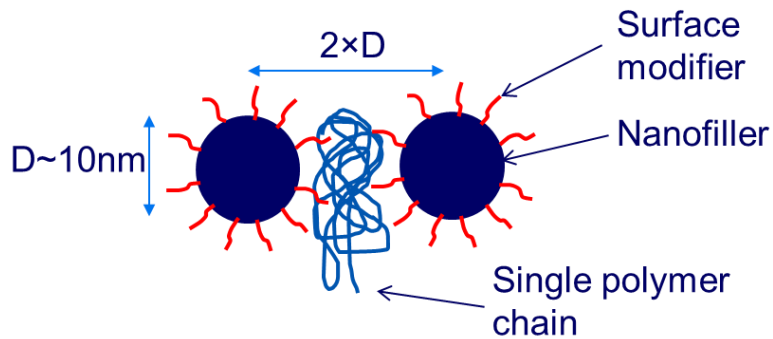
Conformational (C) stress tensor:

$$\hat{\boldsymbol{\sigma}}_C^{(i)} = \frac{1}{J} \left(\hat{\lambda}_N^{(i)} \frac{\partial A_C}{\partial \hat{\lambda}_N^{(i)}} - \frac{1}{3} \sum_{k=1}^3 \hat{\lambda}_N^{(k)} \frac{\partial A_C}{\partial \hat{\lambda}_N^{(k)}} \right) \quad \text{where} \quad A_C = A_C(\hat{\lambda}_N^{(i)}, T, N_s, \alpha, \eta)$$

Stress-induced crystallisation:

$$\hat{\boldsymbol{\sigma}}_C \geq \hat{\boldsymbol{\sigma}}_{C,\text{crit}} \quad \text{where} \quad \hat{\boldsymbol{\sigma}}_{C,\text{crit}} = \hat{\boldsymbol{\sigma}}_{C,\text{crit}}(a_T, a_{s(S)}, \hat{\mathbf{D}})$$

Constitutive model: interface/interphase/gallery



Qiao et al. (2011), 49:740, J. Pol. Phys. B

τ_1

τ_2

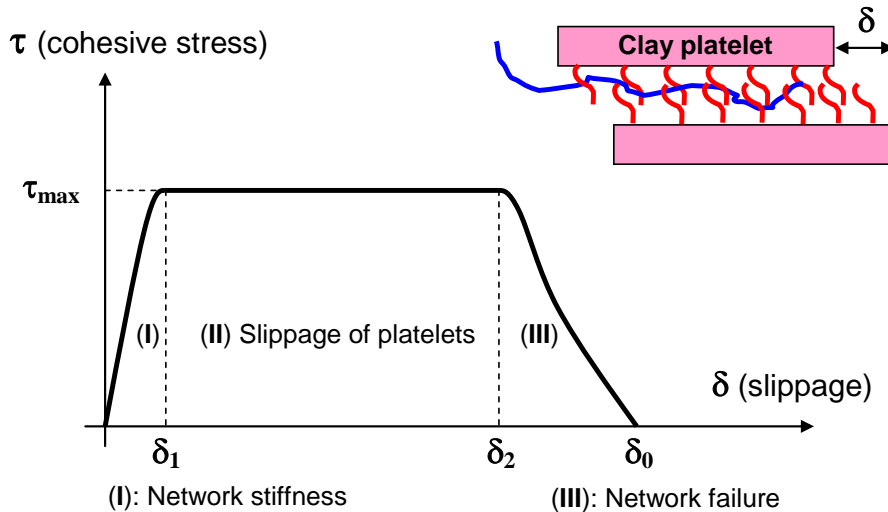
$$\tau_i = \tau_{ref} a_T a_S a_\sigma$$

$$a_T = \exp \left[\left(\frac{\Delta H}{R} \right) \left(\frac{1}{T} - \frac{1}{T_{ref}^{INT}} \right) \right]$$

$$a_S = \exp \left[\frac{C_V}{T_f - T_\infty} - \frac{C_V}{T_{ref}^{INT} - T_\infty} \right]$$

$$\tan \delta_M(\omega_t, T_{ref}^{INT}) = \frac{E_M''(\omega_t, T_{ref}^{INT})}{E_M'(\omega_t, T_{ref}^{INT})}$$

Ł. Figiel/Computational Materials Science 84 (2014) 244-254



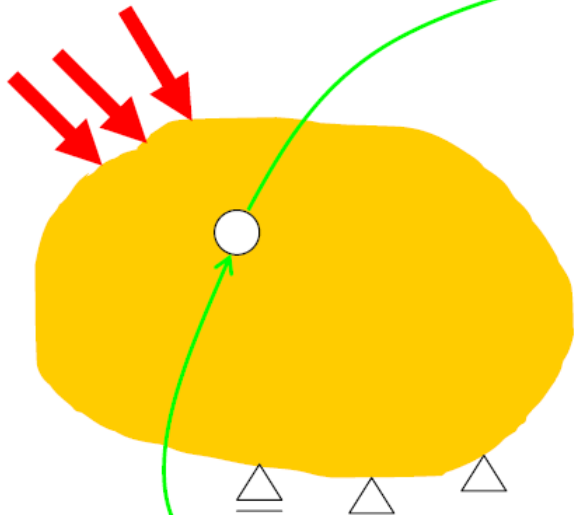
C. Pisano, Ł. Figiel/Composites Science and Technology 75 (2013) 35-41

$$\tau = \tau_{max} f(\delta)$$

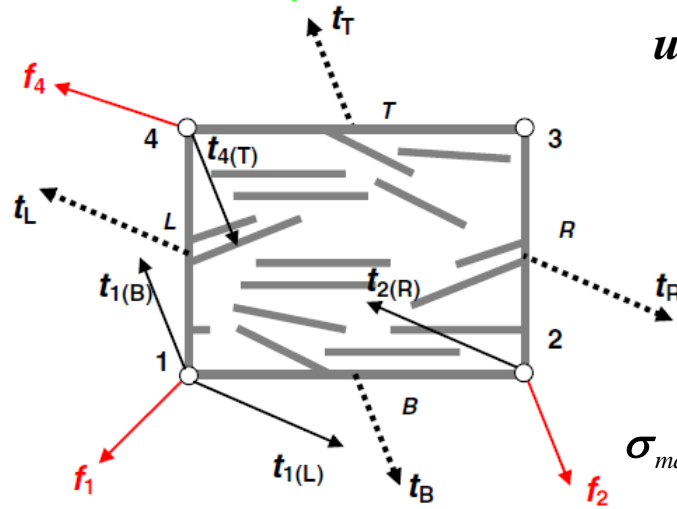
$$\begin{aligned} \text{(I)} \quad f(\delta) &= 2 \frac{\delta}{\delta_1} - \left(\frac{\delta}{\delta_1} \right)^2 && \text{if } \delta < \delta_1; \\ \text{(II)} \quad f(\delta) &= 1 && \text{if } \delta_1 < \delta < \delta_2 \\ \text{(III)} \quad f(\delta) &= 2 \left(\frac{\delta - \delta_2}{\delta_0 - \delta_2} \right)^3 - 3 \left(\frac{\delta - \delta_2}{\delta_0 - \delta_2} \right)^2 + 1 && \text{if } \delta_2 < \delta < \delta_0, \end{aligned}$$

Scale transitions: macro-to-RVE & RVE-to-macro

Macroscopic level



RVE level



Mechanical field

$$\mathbf{u}_{RVE}(\mathbf{x}) = \boldsymbol{\varepsilon}_{macro} \mathbf{X} + \mathbf{u}_f(\mathbf{x})$$

$$\boldsymbol{\varepsilon}_{macro} = \mathbf{F}_{macro} - \mathbf{I}$$



$$\boldsymbol{\sigma}_{macro} = \frac{1}{V_{RVE}} \int_{V_{RVE}} \boldsymbol{\sigma}_{RVE}(\mathbf{x}) dV_{RVE}$$

$$= \frac{1}{V_{RVE}} \int_{\Gamma_{RVE}} \mathbf{t} \otimes \mathbf{x} d\Gamma_{RVE}$$

$$= \frac{1}{V_{RVE}} \sum_{I=1}^N \mathbf{f}_{(I)} \otimes \mathbf{x}_{(I)}$$

Non-mechanical field

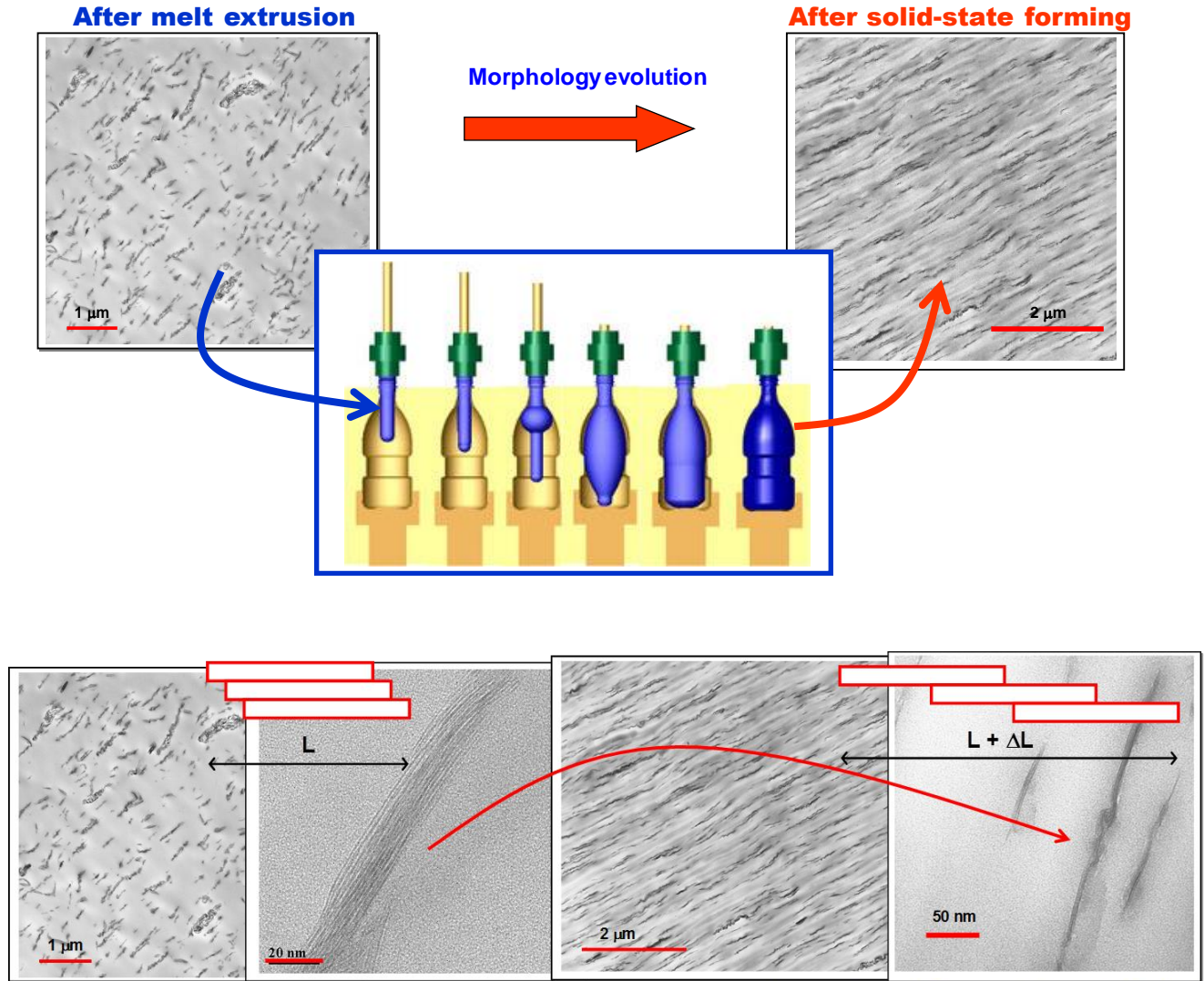
$$\theta_{RVE}(\mathbf{x}) = \theta_{RVE}^{ref} + \nabla_{macro} \theta_{macro} \cdot \mathbf{x} + \theta_f(\mathbf{x})$$

$$q_{RVE} = \frac{1}{V_{RVE}} \int_{V_{RVE}} q_{RVE}(\mathbf{x}) dV_{RVE}$$

Tangent operator

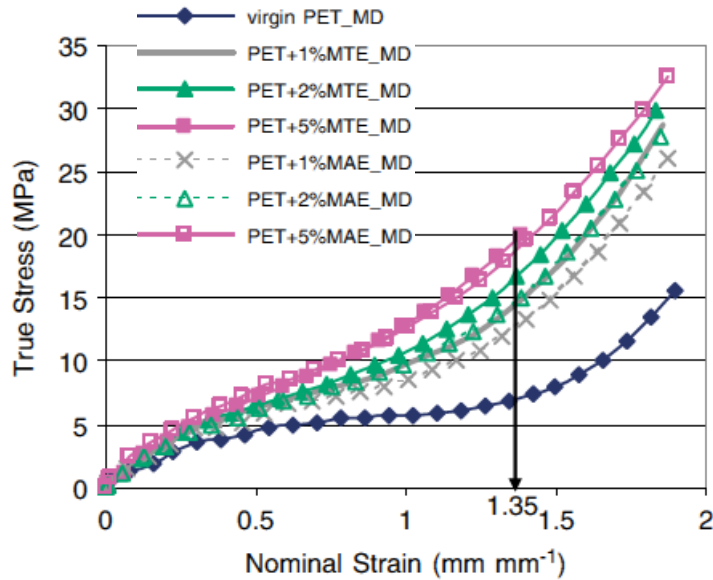
$$\mathbf{C}_{macro} = \frac{\partial \boldsymbol{\sigma}_{macro}}{\partial \boldsymbol{\varepsilon}_{macro}}$$

Case study 1: Secondary processing near T_g

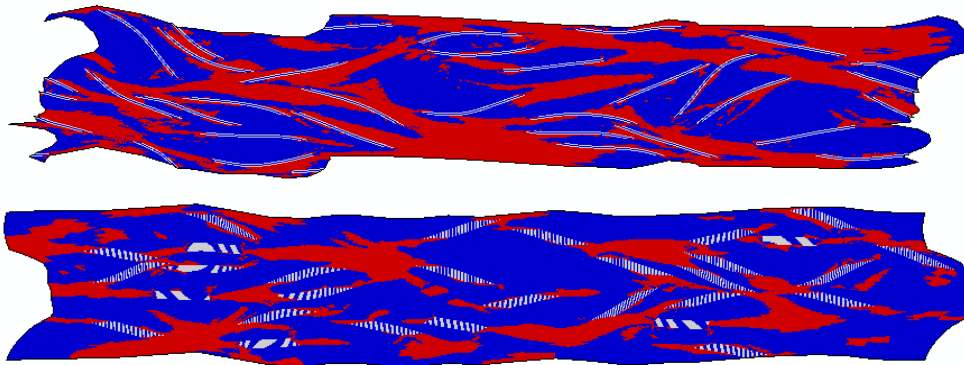


by courtesy of Queens University Belfast

Experiment

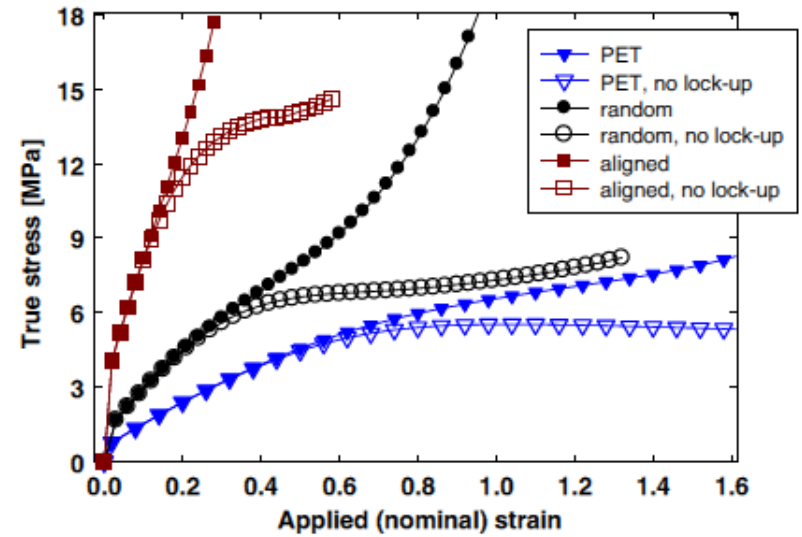
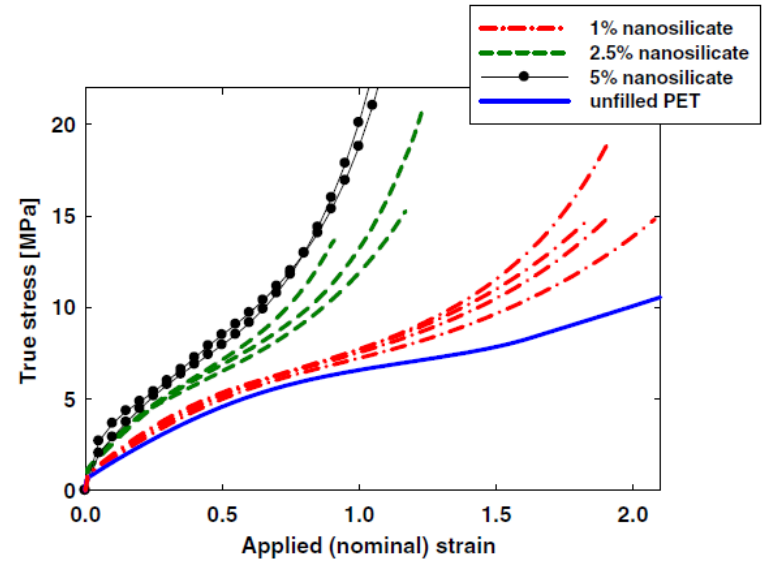


KH Soon et al. *Polym Int* 2009; 58: 1134–1141



■ Viscous flow
■ Stress-induced crystallisation

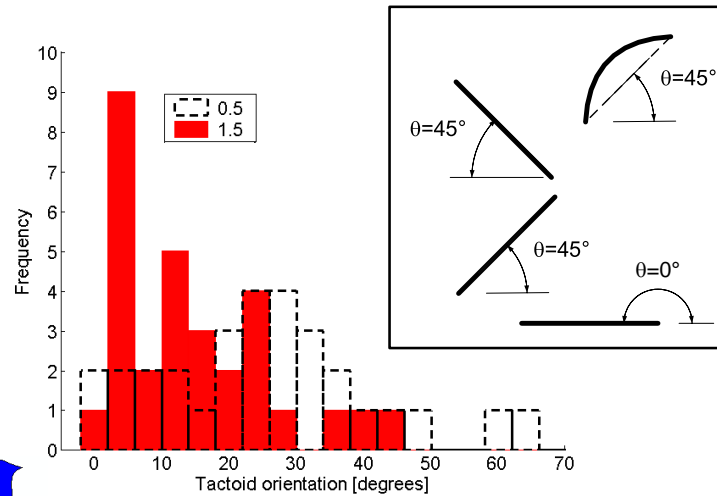
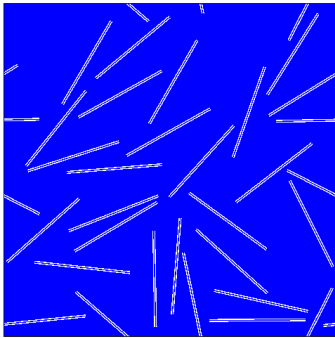
Simulation



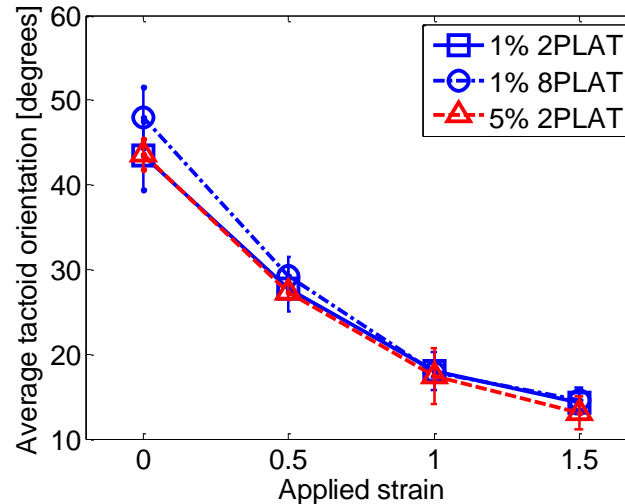
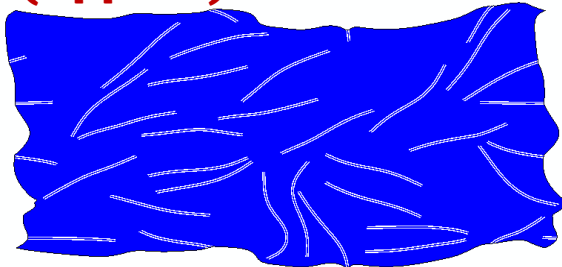
Ł Figiel et al. *Modelling Simul. Mater. Sci. Eng.* 18 (2010) 015001

Morphology evolution with applied deformation

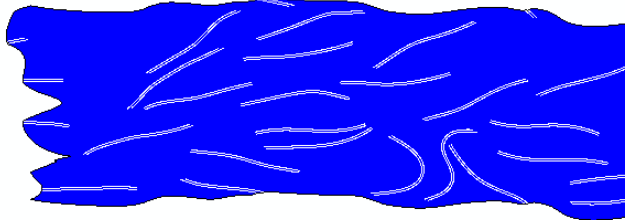
Unstretched



(Applied) Strain ~1

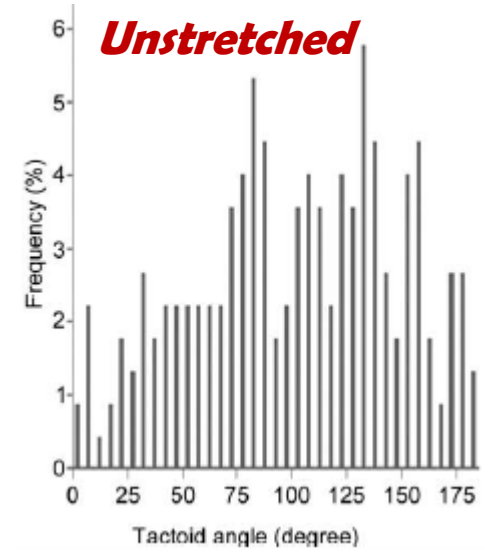


Strain ~1.5

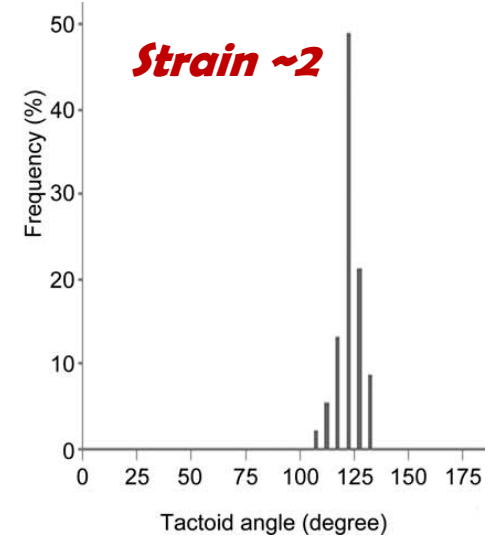


TEM image analysis

Unstretched

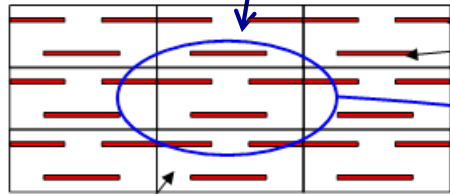
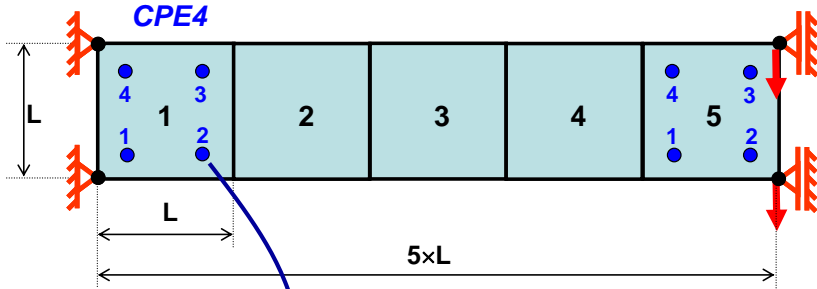


Strain ~2



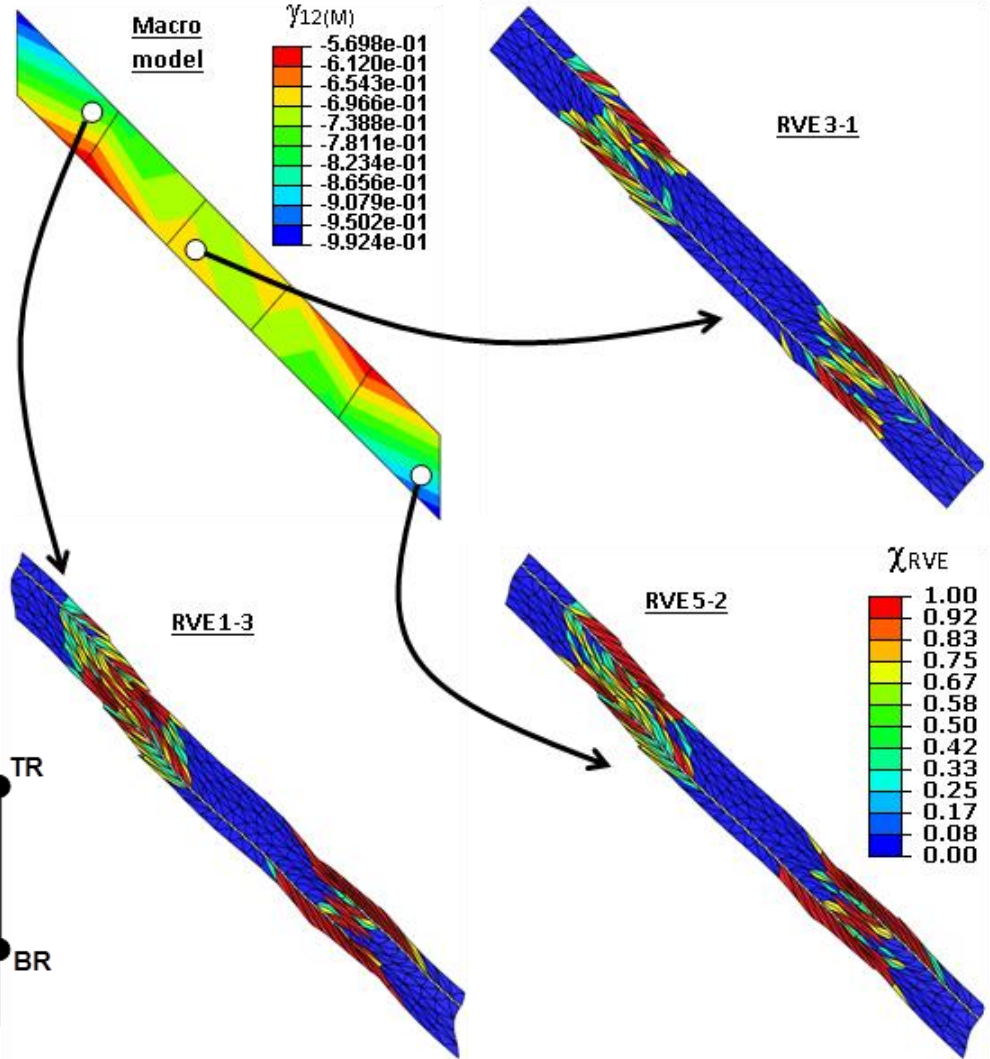
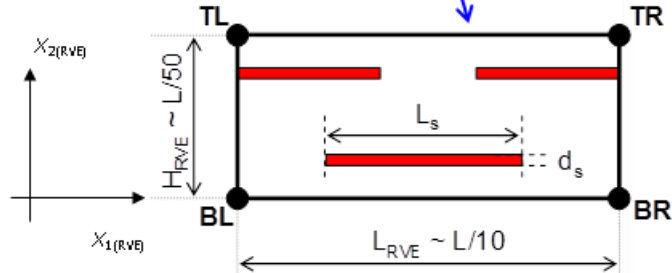
Nanocomposite sheet during thermoforming (100°C , 1s^{-1})

Macro model



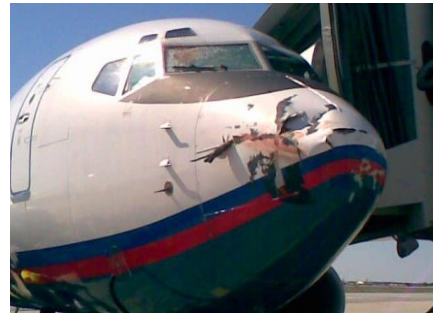
Nanoclay particles

PET matrix



AIP Conf. Proc. 1353, 1226-1231 (2011); doi: 10.1063/1.3589684

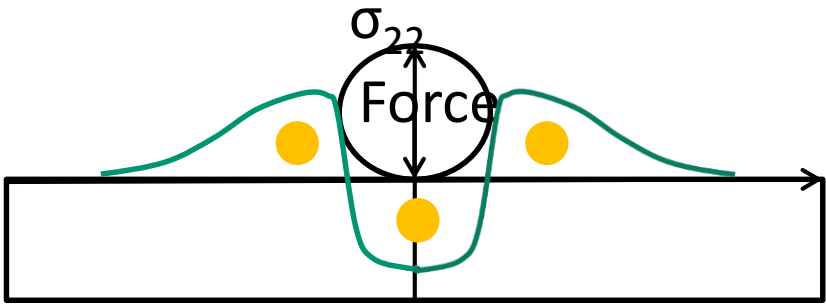
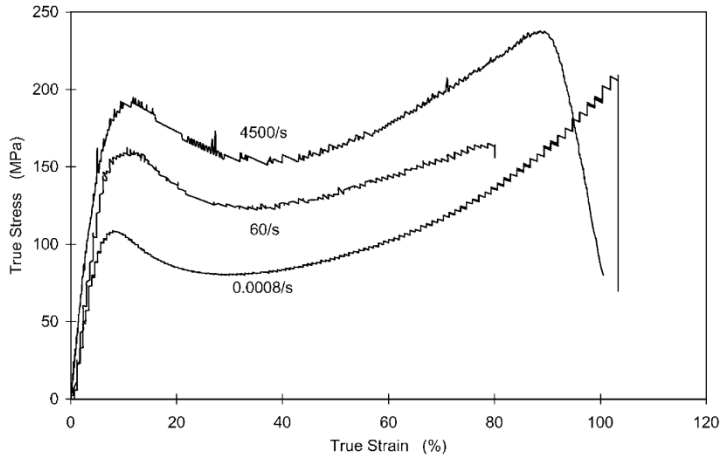
Case study 2: Rate-dependent response



- **CFRP laminates under impact loading**
Opening of matrix cracks (brittle nature of epoxy)
→ delamination at the interfaces, structural degradation

- **Hypothesis: CNT/epoxy surface coating will enhance the impact resistance** due to an increase in energy dissipation/absorption.

(2) CNT enhanced in form of CNT coating of the matrix



MWCNT properties

Elastic constants

$$E_{33}^{\text{zig-zag}} = \frac{4\sqrt{3}C_r}{(r_{\text{CNT}}/2) \left[9 + 3(C_r r_0^2 / C_\theta) / (2\eta_2) \right]}$$

$$\nu_{31}^{\text{zig-zag}} = \frac{-1 + (C_r r_0^2 / C_\theta) / (2\eta_2)}{3 + (C_r r_0^2 / C_\theta) / (2\eta_2)}$$

$$G_{31}^{\text{zig-zag}} = \frac{8\sqrt{3}n^2 \sin^2(\pi/2n) C_r}{(r_{\text{CNT}}/2) \pi^2 (6 + C_r r_0^2 / C_\theta)}$$

$$\eta_2 = \frac{14 + 12\cos(\pi/n) - 2\cos^2(\pi/n)}{10 + 4\cos(\pi/n) - 6\cos^2(\pi/n)}$$

Shen and Li (2004) Phys. Rev. B.

MWCNTs parameters

| | |
|--|-----------------|
| Longitudinal modulus $E_{33}^{\text{tension}}/E_{33}^{\text{compression}}$ (GPa) | 687.21/1051.1 |
| Major Poisson's ratio $\nu_{31}^{\text{tension}}/\nu_{31}^{\text{compression}}$ | 0.12807/0.13686 |
| Longitudinal shear modulus G_{31} (GPa) | 204.71 |
| In-plane bulk modulus K_{12} (GPa) | 112.11 |
| In-plane shear modulus G_{12} (GPa) | 2.0256 |

Weidt & Figiel (2015), 115: 52, Comp. Sci. Techn.

e.g. C_r bond-stretching constant; C_θ bond-angle variation constant; n - chirality

Matrix behaviour

Strain energy function

$$A_C = A_C(\hat{\lambda}_N^{(i)}, T, N_C, \alpha)$$

Edwards & Vilgis (1986), 27: 483, Polymer

Rejuvenation

$$T_{f\sigma} = T_{f\sigma 0} + (T_{f\sigma\infty} - T_{f\sigma 0}) \left[1 - \exp\left(-\frac{\bar{\epsilon}^v}{\epsilon_0^v}\right) \right]$$

Buckley et al. (2004), 52: 2355, J. Mech. Phys. Sol.

Adiabatic heating

$$\dot{T} = \frac{1}{\rho c} \left[\bar{\sigma} : \bar{D} - \bar{\sigma}^b : \bar{D}^e \right] - \frac{\varphi \Delta c \dot{T}_{f\sigma}}{c}$$

Buckley et al. (2004), 52: 2355, J. Mech. Phys. Sol.

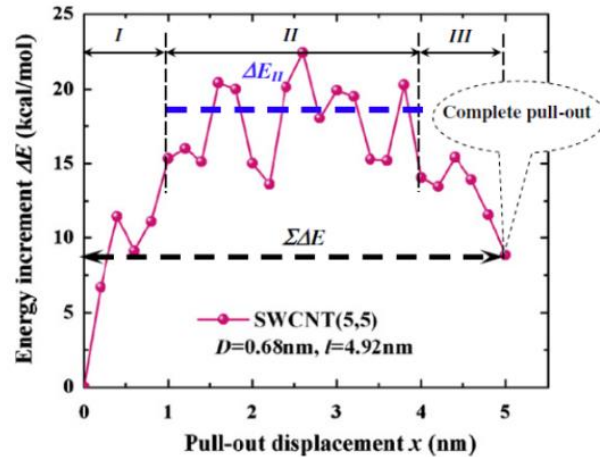
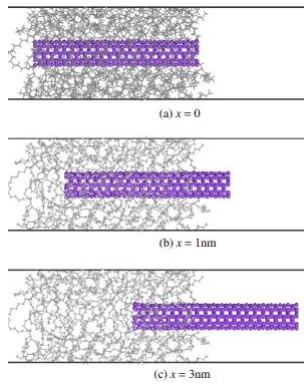
Values of model parameters

| | Epon 828/Jeffamine T403 |
|---|-------------------------|
| Shear modulus G (Pa) | 0.87e+9 |
| Bulk modulus K (Pa) | 3.078e+9 |
| Glass transition temperature T_g (K) | 363 ^a |
| Density ρ (kg m ⁻³) | 1140 ^a |
| Number density of crosslinks N_c (m ⁻³) | 5.7e+27 |
| Inextensibility factor of network α | 0.297 |
| Final fictive temperature $T_{f\sigma\infty}$ (K) | 372 |
| Linear viscoelastic relaxation time τ_0 (s) | 2.02e+6 |
| Rejuvenation strain range ϵ_0^v | 0.339 |

Weidt & Figiel (2015), 115: 52, Comp. Sci. Techn.

Interface behaviour

CNT pull-out via MD

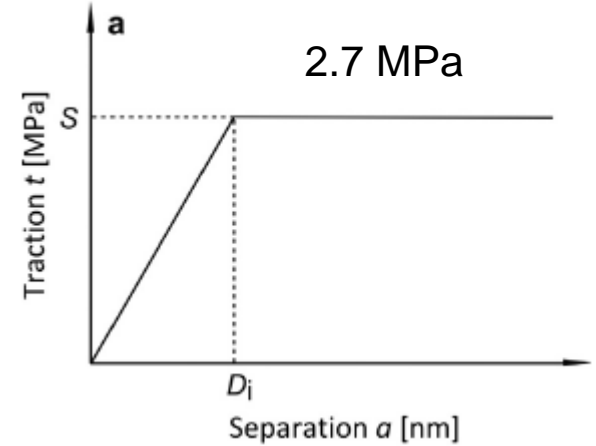


$$F_{\max}^{II} = \frac{\langle \Delta E^{II} \rangle}{\langle \Delta x^{II} \rangle}$$



$$S = \frac{F_{\max}^{II}}{\pi dl}$$

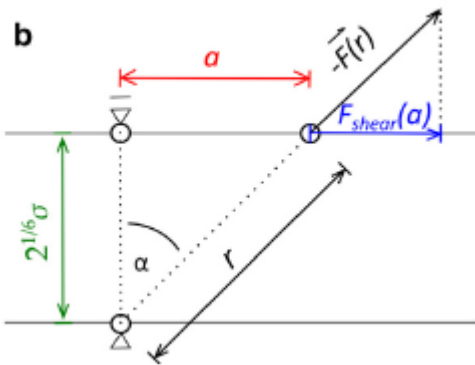
Tangential traction-separation law



Li et al. (2011), 50: 1854, Comp. Mat. Sci.

$$r^2 = a^2 + (2^{1/6} \sigma)^2$$

Weidt & Figiel (2015), 115: 52, Comp. Sci. Techn.



$$F(r) = 4 \frac{\epsilon}{r} \left[12 \left(\frac{\sigma}{r} \right)^{12} - 6 \left(\frac{\sigma}{r} \right)^6 \right]$$

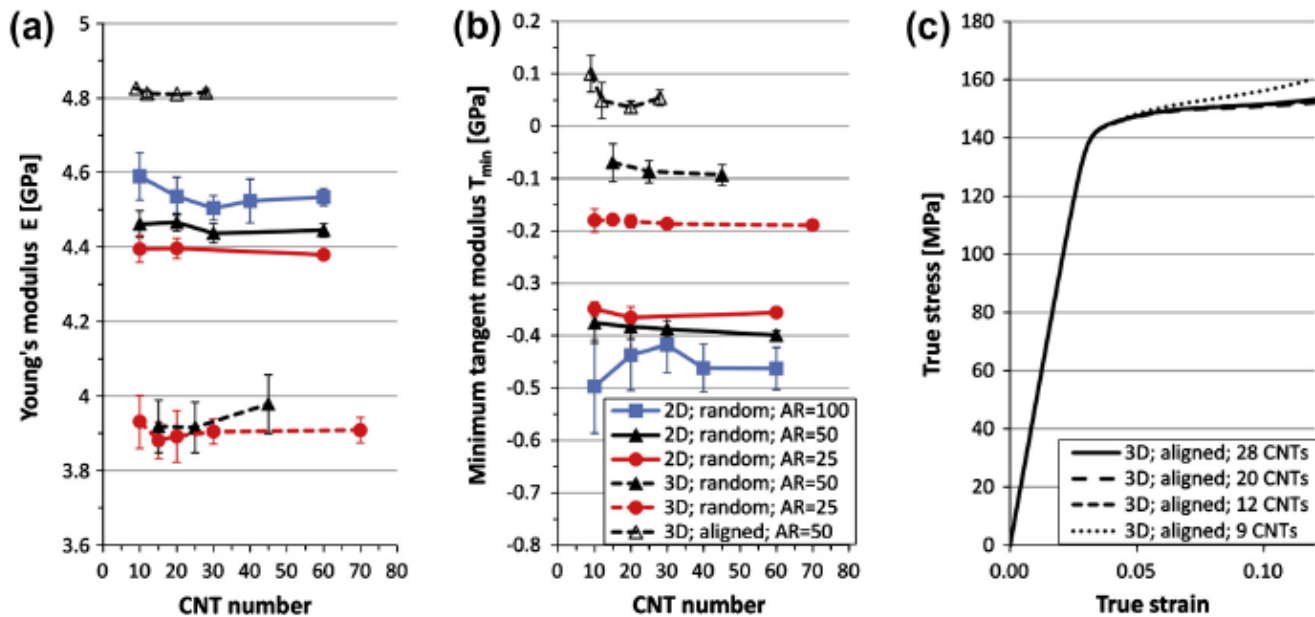
$$F_{\text{shear}} = -F \sin \alpha \text{ with } \alpha = \arccos \left(\frac{2^{1/6} \sigma}{r} \right) \text{ and } r^2 = a^2 + (2^{1/6} \sigma)^2$$

$$F_{\text{shear}}(a) = -4 \frac{\epsilon a}{a^2 + 2^{1/3} \sigma^2} \left[12 \frac{\sigma^{12}}{(a^2 + 2^{1/3} \sigma^2)^6} - 6 \frac{\sigma^6}{(a^2 + 2^{1/3} \sigma^2)^3} \right]$$

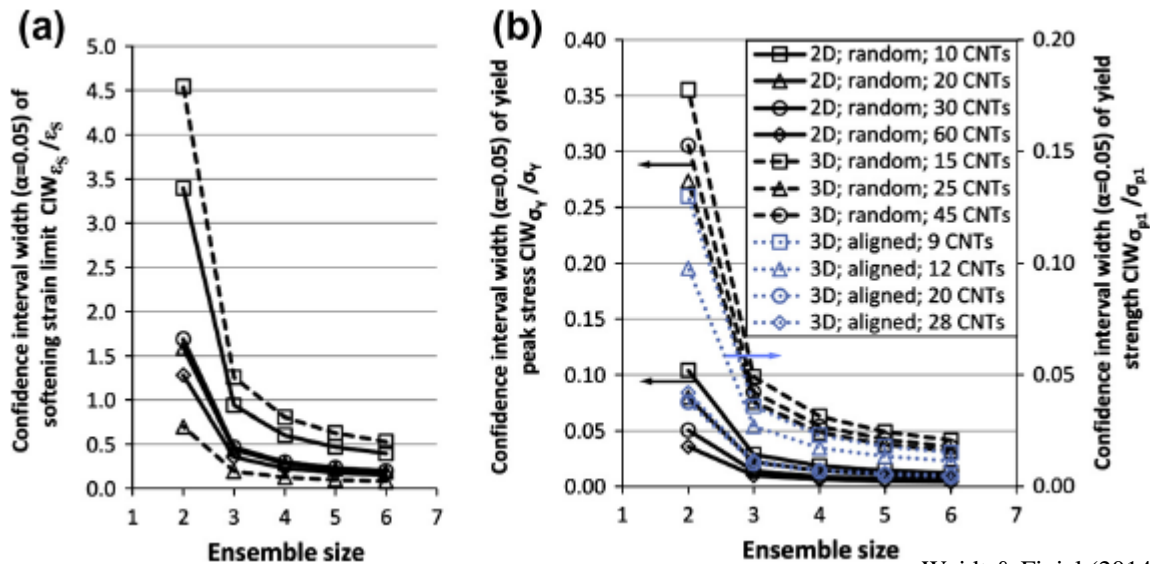
$$D_i (F_{\text{shear}}^{\max}(a)) = 0.225 \text{ nm}$$

Weidt & Figiel (2015), 115: 52, Comp. Sci. Techn.

RVE size:

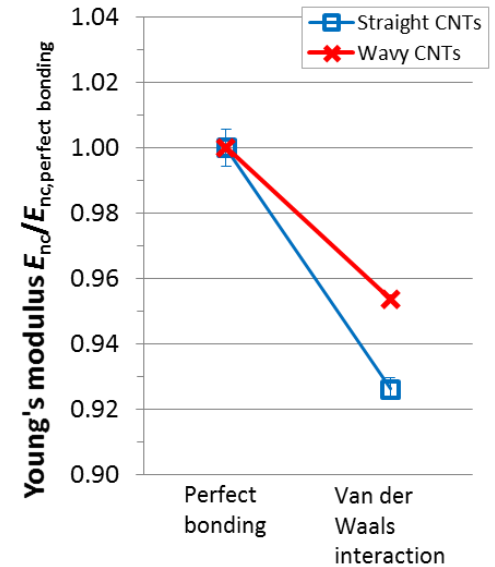
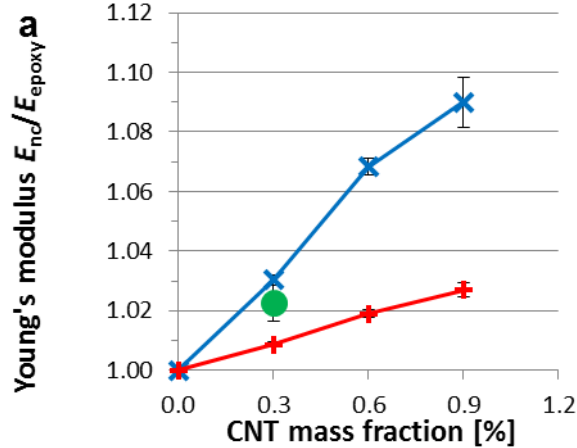
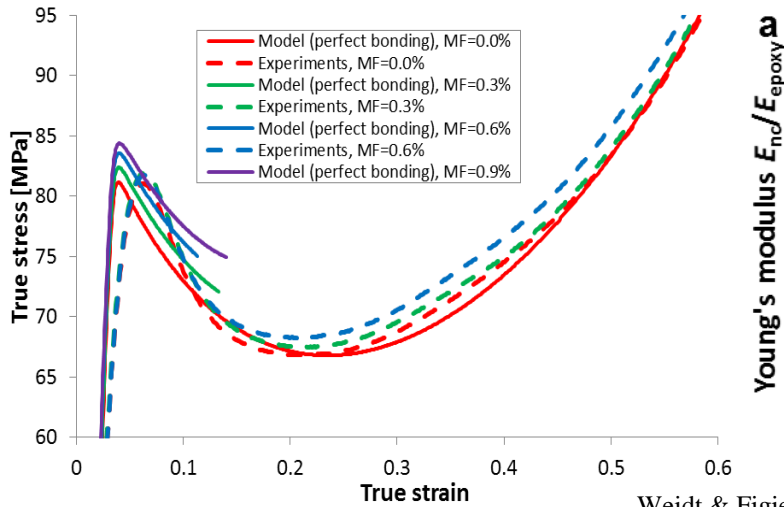


Ensemble size:



Weidt & Figli (2014), 82: 298, Comp. Mat. Sci.

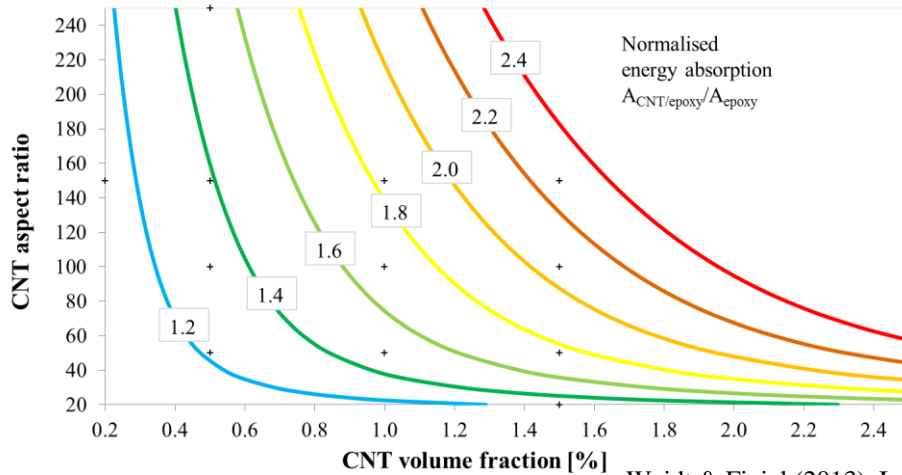
Stress-strain rate response, and related parameters



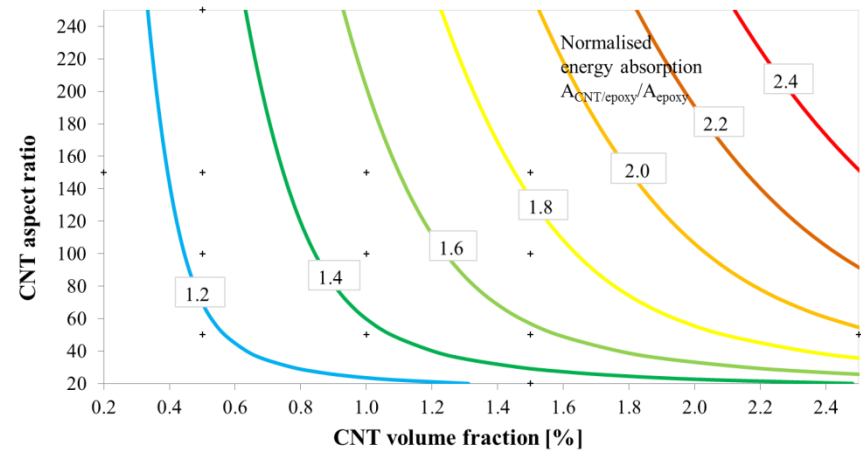
Weidt & Figiel (2015), 115: 52, Comp. Sci. Techn.

Energy absorption

Quasi-static rate ($1 \times 10^{-3} \text{ s}^{-1}$)



Impact rate ($1 \times 10^3 \text{ s}^{-1}$)



Weidt & Figiel (2013), In. Njuguna (Ed.), Structural Nanocomposites, 207-224, Springer, 2013.

Concluding remarks

- Computationally-efficient & accurate, multiscale approach can assist in the optimisation of processing and property enhancements for polymer nanocomposites
- Further work ongoing on:
 - Linking with molecular simulations to account more *accurately* for nanoparticle functionalization & nanoparticle-polymer interactions
 - Description of nanoparticle functionalization-related *uncertainty*
 - Computational efficiency enhancement for localisation-homogenisation scheme through model *reduction* and parallel processing
 - Incorporation of *non-mechanical fields* (e.g. thermal, electric) into the scheme

Acknowledgements

- Dr. C. Pisano, Dr. D. Weidt (University of Limerick, Ireland)
- Prof. P. Buckley (University of Oxford, UK)
- Prof. F. Dunne (Imperial College London, UK)
- Dr. P. Spencer (University of Bradford, UK)
- Dr. G. Menary (Queen's University Belfast, UK), Dr. K. Soon, Dr. R. Rajeev (formerly at Queen's University Belfast, UK)
- Prof. A. Galeski (CMMS Lodz, Poland)

- Engineering and Physical Sciences Research Council (EPSRC), UK
- Materials & Surface Science Institute, University of Limerick, Ireland
- Irish Research Council (IRC)
- Irish Centre for High-End Computing (ICHEC)
- National Science Centre, Poland